

# Ductility Analysis of Re-entrant Corner Reinforced Concrete Buildings Using Nonlinear Time History Analysis

Joshua C. Junio<sup>1</sup>

<sup>1</sup>Faculty, Civil Engineering Department, Pangasinan State University- Urdaneta City, Pangasinan, Philippines

\*\*\*

**Abstract** - This study investigates the ductile behavior of re-entrant corner reinforced concrete (RC) buildings using nonlinear time history analysis. Re-entrant corners introduce geometric irregularities that significantly influence seismic performance, particularly the structural ductility, which is a critical factor in energy dissipation and collapse prevention during earthquakes. A total of 180 two-storey RC buildings with various plan shapes and re-entrant projections were modeled and designed using SAP2000, following NSCP 2015 provisions. Nonlinear time history analysis was performed using the 1995 Kobe earthquake ground motion. Ductility values in both  $x$  and  $y$  directions were calculated by bilinearizing the base shear-displacement curves and relating peak ground acceleration (PGA) at yield and ultimate states. To estimate ductility values, stepwise nonlinear regression analysis was conducted in MATLAB, utilizing models such as polynomial regression, support vector regression, Gaussian process regression, decision trees, ensemble methods, and neural networks. Twelve input variables, including plan shape, re-entrant corner projection ( $x$  and  $y$ ), building weight, material properties (concrete and rebar), shear reinforcements (beams and columns), and flexural reinforcement in columns, top and bottom bar reinforcement in beams, and compression-to-tension reinforcement ratio in beams, were evaluated. The best-performing models were identified based on  $R^2$ , RMSE, MAE, and MSE. A regression model was then applied to predict the ductility of an actual re-entrant corner RC building, which was validated through nonlinear pushover and time history analysis. The study presents a reliable framework for estimating ductility in irregular RC buildings and offers valuable insights for enhancing seismic design and safety in earthquake-prone regions.

**Key Words:** Re-entrant Corner Irregularity, Reinforced Concrete (RC) Buildings, Nonlinear Time History Analysis, Regression Analysis

## 1. INTRODUCTION

The Philippines, due to its location, is prone to earthquakes, experiencing around 30 daily [1]. Historical earthquakes like the 1976 Moro Gulf (M8.1) and the 1990 Luzon quake (M7.8) have caused severe damage and fatalities [2]. Earthquake impacts are worsened by structural vulnerabilities, particularly a lack of structural ductility, the ability of a building to deform without collapsing. Incorporating

ductility helps structures absorb seismic energy and minimize collapse risks [3][4]. Among RC buildings, re-entrant corner configurations are common for their spatial and aesthetic efficiency, but their geometric irregularity increases seismic vulnerability which leads to stress concentration and torsion [5]. Per the NSCP 2015, re-entrant corner irregularity is defined when projections exceed 15% of the plan dimension [6]. This irregularity significantly affects seismic parameters such as base shear and storey drift, which influence ductility and the response modification factor (R) [7][8]. However, ATC-19 do not fully address plan irregularities, and adjustments are recommended for irregular structures [9][10]. Ductility can be improved with proper materials, reinforcement, and joint detailing [11]. While numerical simulations and static/ dynamic analyses are standard, they often demand high computational resources [12]. To address this, this study proposes using nonlinear time history analysis and regression analysis to estimate ductility values in re-entrant corner RC buildings. The goal is to develop a more efficient, data-driven framework to assess the seismic performance of irregular RC structures, enhancing safety and resiliency in building design.

### 1.1 Statement of the Objectives

This study aims to assess the ductile behavior of re-entrant corner reinforced concrete (RC) buildings and to estimate the ductility considering plan shape, projection beyond a re-entrant corner along  $x$ -direction and  $y$ -direction, building weight, material properties, shear reinforcement in beams and columns, flexural reinforcement in columns, top and bottom bar reinforcement in beams, and compression-to-tension reinforcement ratio in beams using regression analysis. Specifically, the study sought answers:

- To evaluate the seismic response of re-entrant corner RC buildings using time history analysis considering the effect of the following parameters on the ductility for the development of a regression model:
  - plan shape,
  - projection beyond a re-entrant corner along  $x$  and  $y$  direction,
  - building weight,
  - material properties,
  - shear reinforcement in beams and columns,
  - flexural reinforcement in columns,
  - top and bottom bar reinforcement in beams, and

- compression-to-tension reinforcement ratio in beams.
- To develop a regression model for estimating the ductility of re-entrant corner RC buildings.
- To validate the ductility of an actual re-entrant corner RC building using the developed regression model and the code-prescribed methods.

## 2. METHODOLOGY

### 2.1 Evaluation of the Seismic Response of Re-entrant Corner RC Buildings

- **Structural Modeling and Design of the 180 Building Models**

The study analyzed two-storey RC buildings with a regular storey height of 3.0 m. The study models include 3D irregular RC buildings in U-shaped, E-shaped, H-shaped, L-shaped, Plus-shaped, T-shaped, and Z-shaped plans. The building inventory also includes a regular (box-shaped) building.

Five different projections, 0%, 20%, 40%, 60%, and 80%, were studied. A total of 45 building models with unique plan shapes were modeled and designed using SAP2000. The different building model parameters are shown in Table 1.

**Table - 1: Building Models Parameters**

Parameter	Value
Building height	6.0 m
Storey height	3.0 m
Number of floors	2
Span length	4.0 m
Re-entrant corner projections	0%, 20%, 40%, 60%, 80%
Plan Configuration	Regular, E, H, L, P, T, U, Z

The different material properties used in the building models are shown in Table 2.

The forty-five (45) building models were categorized into four (4) cases based on the material properties, as shown in Table 3. A total of one hundred eighty (180) building models were designed and analyzed in this study.

**Table - 2: Material Properties**

Property	Value
Concrete strength, $f_c'$	25 MPa, 28 MPa
Modulus of elasticity of concrete, $E_c$	200000 MPa
Yield strength of steel	280 MPa, 420 MPa

**Table - 3: Building Model Cases Based on Material Properties**

Cases	$f_c', f_y$
Case 1	25 MPa, 280 MPa
Case 2	28 MPa, 280 MPa
Case 3	25 MPa, 420 MPa
Case 4	28 MPa, 420 MPa

The beams and columns were designed with equal dimensions in all building models, as shown in Table 4. Three-dimensional frame modeling and analysis were conducted for the 180 building models using the software SAP2000.

**Table - 4: Dimensions of Frame Models**

Case	Material Property	Beam Dimensions (mm)	Column Dimensions (mm)
Case 1	25 MPa, 280 MPa	300 x 400	360 x 360
Case 2	28 MPa, 280 MPa	300 x 400	360 x 360
Case 3	25 MPa, 420 MPa	300 x 400	360 x 360
Case 4	28 MPa, 420 MPa	300 x 400	360 x 360

The gravity loads used are presented in Table 5, and the lateral loads were computed using SAP2000, according to UBC 97. Linear static analysis and response spectrum analysis were utilized for designing the structural members. The complete seismic parameters used in the analysis are shown in Table 6.

**Table - 5: Loads on the Building Models**

Load	Value
DEAD LOADS, DL	<b>5.46 kPa</b>
Slab	<b>3.54 kPa</b>
Floor Finish, FF	<b>1.58 kPa</b>
Ceiling Finish, CF	<b>0.14 kPa</b>
Mechanical, Electrical, Plumbing, MEP	<b>0.2 kPa</b>
LIVE LOADS, LL	<b>4.8 kPa</b>
DL <sub>UDL</sub>	<b>7.28 kN/m</b>
LL <sub>UDL</sub>	<b>6.4 kN/m</b>
ADDITIONAL LOAD FOR WALL (DL)	<b>7.6 kN/m</b>
LATERAL LOAD	<b>UBC 97</b>

**Table - 6: Seismic Parameters**

Parameter	Value
Seismic zone factor	<b>0.4</b>
Seismic source type	<b>A</b>
Importance factor	<b>1.0</b>
Soil profile type	<b>SD</b>
Distance from a seismic source	<b>≤ 2 km</b>
Near Source Factor, Na and Nv	<b>1.5 and 2.0</b>
Seismic Response Coefficient, Ca and Cv	<b>0.66 and 1.28</b>
Numerical Coefficient, Ct	<b>0.0731</b>
Seismic Response Factor R	<b>8.5</b>

The 180 buildings were designed until all beams and columns had equal dimensions. The largest shear reinforcement requirement in beams and columns, largest value of flexural reinforcement in columns, and largest compression-to-tension reinforcement ratio in beams were obtained from the results of each building model.

These quantities served as input values in the development of a regression model for estimating the ductility factor.

• **Performing Nonlinear Time History Analysis**

Ground motion data from the 1995 Kobe Earthquake in Japan was selected for the analysis. The parameters used to download and filter the ground motion from the PEER Ground Motion Database are summarized in Table 7.

**Table - 7: 1995 Kobe Earthquake in Japan**

Parameter	Value
Magnitude	<b>6.9</b>
Mechanism	<b>Strike slip</b>
Rjb	<b>22.5 km</b>
Rrup	<b>22.5 km</b>
Vs30	<b>312 m/sec</b>

The horizontal components of the recorded seismic event were both exported to Microsoft Excel and subsequently imported into SAP2000 to define a time history function. The data was scaled to peak ground acceleration (PGA) ranging from 0.1g to 4.0g to simulate varying levels of earthquake intensity.

Nonlinear Time History Analysis was conducted for each model. Key response parameters were extracted including base shear and maximum roof displacement. Results were graphed to visualize the relationships between PGA and structural response parameters.

Similar process was applied for the nonlinear time history analysis of the actual re-entrant corner RC building.

• **Calculation of Ductility Values of the 180 Building Models**

The graph of base shear versus maximum roof displacement was used two critical response points, including maximum point and yield point of each building model. A curve fitting technique was applied to identify the maximum point, while the yield point was determined using bilinear approximation, as shown in Figure 1.

A graph of peak ground acceleration (PGA) against displacement was also generated as shown in Figure 2. The PGA at maximum and PGA at yield is obtained from this graph. The ductility values on both directions were obtained by dividing the PGA at the maximum response of the building by the PGA at the yield point.

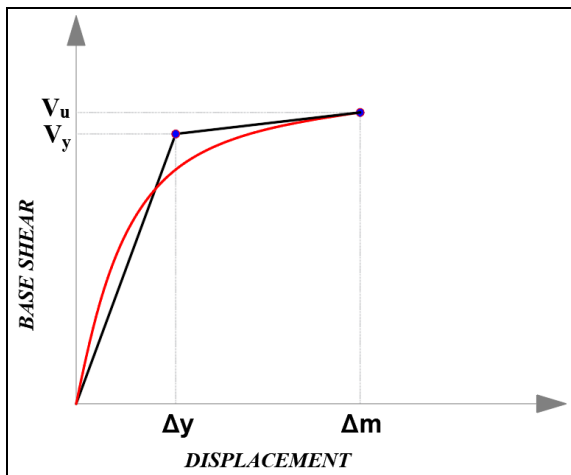


Fig - 1: Bilinear Approximation of Base Shear versus Displacement

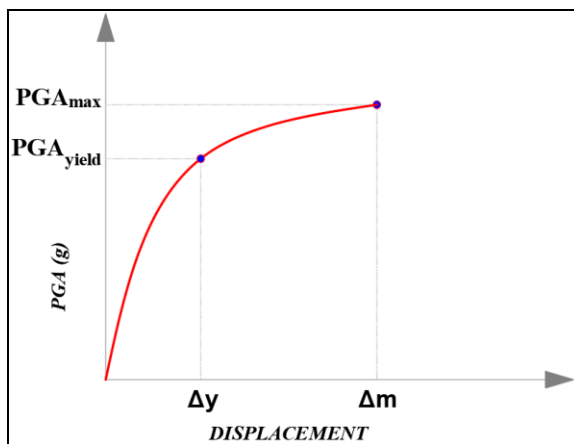


Fig - 2: PGA versus Displacement

• **Relationship of the Various Parameters on the Ductility**

The dataset was prepared by organizing the independent variables (IVs) and dependent variables. Modeling began by using only two IVs and incrementally increase the number of IVs up to a full model with twelve IVs.

How each additional variable affects model performance was assessed. For every IV count, train multiple nonlinear regression models to capture various data relationships.

For each trained model, the performance was evaluated using coefficient of determination  $R^2$ , root mean squared error RMSE, mean absolute error MAE, and mean squared error MSE. The process was repeated separately for ductility in the x-direction and y-direction.

**2.2 Development of a Regression Model for Estimating the Ductility Factor of Re-entrant Corner RC Buildings**

• **Dataset Preparation**

The 12 input features derived from the structural analysis and design of the 180 building models were collected and prepared.

These include plan shape, projection beyond re-entrant corner along x-direction and y-direction, building weight, material properties (concrete and rebar strength), shear reinforcement in beams and columns, flexural reinforcement in columns, top bar and bottom bar reinforcement in beams, and compression-to tension reinforcement ratio in beams. The target output variable was defined: Ductility (X and Y direction), obtained from nonlinear time history analysis.

• **Modeling using MATLAB’s Regression Learner App**

The dataset was loaded into Regression Learner App. The dataset was split into training and validation sets to ensure model generalizability.

Various regression algorithms were applied: linear regression, regression trees, support vector machines (SVM), Gaussian process regression (GPR), and ensemble methods. Hyperparameter optimizations were performed using cross validation.

Model performance was evaluated using the following metrics: Root Mean Square Error, R-squared, and Mean Absolute Error. Regression models were tabulated and ranked based on their performance.

• **Modeling using MATLAB’s Neural Network Fitting App**

Neural Network Fitting App from the Deep Learning Toolbox was used to build regression models. The modeling process was divided into three categories: Ductility in the X-direction, Ductility in the Y-direction, and Ductility in both directions. Multiple regression models were developed for each category using the specifications in Table 8.

**Table - 8: Neural Network Fitting App Specifications**

Specification	Value
Input data (predictors)	<b>12 features</b>
Target data (output)	<b>1 output</b>
Training data	<b>75%, 80%</b>
Validation data	<b>15%, 10%</b>
Testing data	<b>15%, 10%</b>
Number of Hidden Neurons	<b>1, 2, 3, 4, 5, 6, 7, 8, 9, 10</b>
Training algorithm	<b>Levenberg-Marquardt</b>

### 2.3 Ductility Analysis of the Actual Re-entrant Corner RC Building

- Actual Re-entrant Corner RC Building Description and Structural Modeling**

The complete architectural and structural plans of the actual building used in this study was obtained from the Department of Public Works and Highways (DPWH) database.

A two-storey building with a T-shaped plan was selected for the study. The structural and earthquake parameters used is in Table 9 and 10, respectively.

**Table – 9:** T-shaped Building Structural Parameters

Parameter	Value
Concrete strength, $f_c'$	<b>25 MPa (3500 psi)</b>
Modulus of elasticity of concrete, $E_c$	<b>200000 MPa</b>
Yield strength of steel	<b>280 MPa</b>
Total Floor Slab Loading (DL)	<b>4.5 kPa</b>
Live Loads (LL)	
Office/ Faculty Lounge	<b>2.90 kPa</b>
Restrooms	<b>2.40 kPa</b>
Corridors above, stairs	<b>3.80 kPa</b>
Load For Exterior Wall	<b>7.64 kN/m</b>
Lateral Load	<b>UBC 97</b>

**Table – 10:** T-shaped Building Seismic Parameters

Parameter	Value
Seismic zone factor	<b>0.4</b>
Seismic source type	<b>A</b>
Importance factor	<b>1.0</b>
Soil profile type	<b>SD</b>
Distance from a seismic source	<b>≤ 2 km</b>
Near Source Factor, $N_a$ and $N_v$	<b>1.5 and 2.0</b>
Seismic Response	<b>0.66 and 1.28</b>

Coefficient, $C_a$ and $C_v$	
Numerical Coefficient, $C_t$	<b>0.0731</b>
Seismic Response Factor R	<b>8.5</b>

The building was modeled in SAP2000 using the data obtained from the plans and specifications. The same model was used for nonlinear pushover analysis, nonlinear time history analysis, and for extracting inputs to the regression model.

- Nonlinear Analyses of the Actual Building**

Conducted nonlinear pushover analysis to determine maximum displacement  $\Delta m$  and yield displacement  $\Delta y$ .

Calculated ductility  $\mu$  by dividing maximum displacement by  $\Delta m$  and yield displacement  $\Delta y$ .

Nonlinear time history analysis was also conducted using the 1995 Kobe Japan earthquake ground motion data. Ductility was computed by dividing the PGA at max divided by PGA at yield state.

- Comparison and Model Validation**

The developed regression model was applied to estimate the ductility of the actual building. The predicted ductility was compared with the ductility obtained through nonlinear pushover analysis and nonlinear time history analysis.

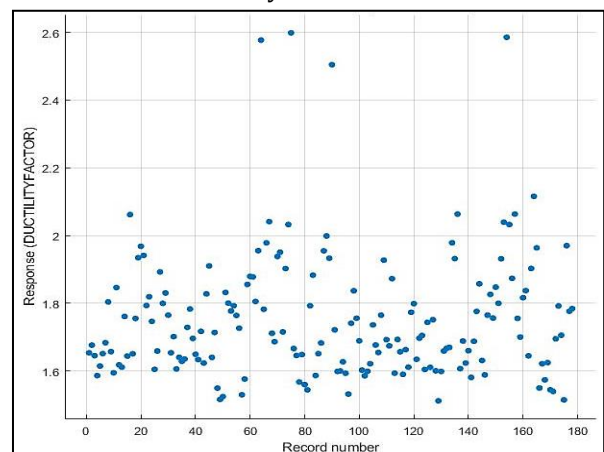
This comparison was conducted to validate the accuracy and reliability of the regression-based estimation approach.

### 3. RESULTS

#### 3.1 Evaluation of the Seismic Response of Re-entrant Corner RC Buildings

Shown in Charts 1 and 2 are the ductility values in the X and Y direction of the 180 building models.

**Chart – 1:** Ductility Values in the X direction



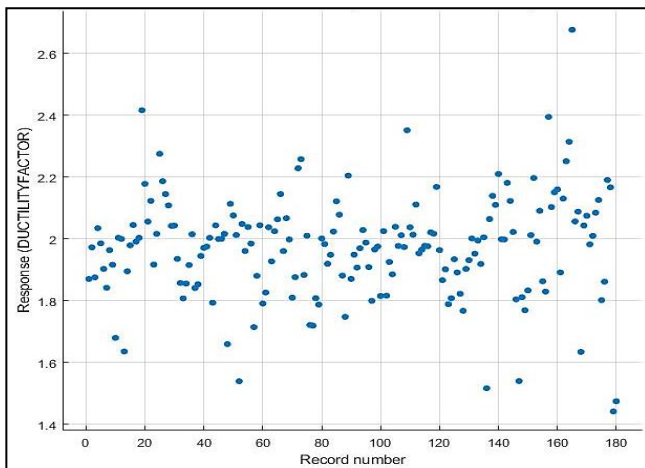


**Chart - 2:** Ductility Values in the Y direction

The highest and lowest ductility in the X direction and Y direction are shown in Tables 11 and 12.

**Table - 11:** Highest and Lowest Ductility Values at X Direction

Case	Model Name	Ductility (Highest)	Model Name	Ductility (Lowest)
Case 1	L4080_ FC25FY280	<b>2.062</b>	E6020_ FC25FY280	<b>1.586</b>
Case 2	T4080_ FC25FY420	<b>2.599</b>	E6020_ FC25FY420	<b>1.516</b>
Case 3	Z4060_ FC28FY280	<b>1.979</b>	Z2020_ FC28FY280	<b>1.512</b>
Case 4	L8080_ FC28FY420	<b>2.586</b>	Z2040_ FC28FY420	<b>1.515</b>

**Table - 12:** Highest and Lowest Ductility Values at Y Direction

Case	Model Name	Ductility (Highest)	Model Name	Ductility (Lowest)
Case 1	L8080_ FC25FY280	<b>2.416</b>	L2080_ FC25FY280	<b>1.636</b>
Case 2	T4040_ FC25FY420	<b>2.258</b>	H2040_ FC25FY420	<b>1.540</b>

Case 3	L8080_ FC28FY280	<b>2.351</b>	U6080_ FC28FY280	<b>1.768</b>
Case 4	T4080_ FC28FY420	<b>2.676</b>	Z4060_ FC28FY420	<b>1.442</b>

Shown in Charts 3 and 4 are the fitted curve for the base shear and roof displacement values from the results of the nonlinear time history analyses of the building model T4080 in X and Y directions. The maximum point was determined from this graph.

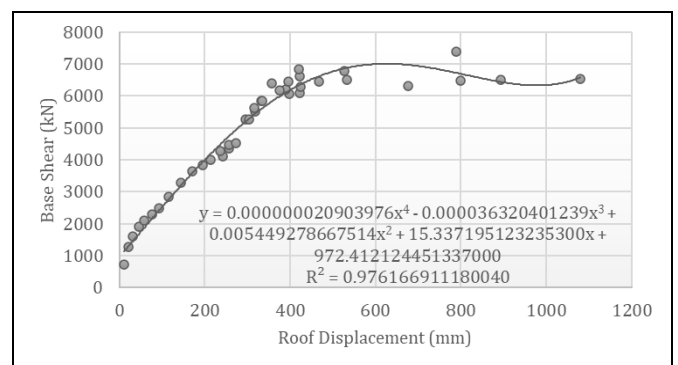


**Chart - 3:** Base Shear Versus Displacement of T4080\_FC25FY420 (X Direction)

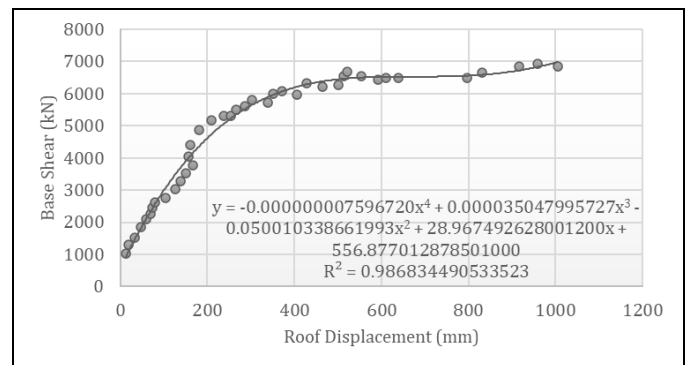


**Chart - 4:** Base Shear Versus Displacement of T4080\_FC25FY420 (Y Direction)

The bilinearization using Microsoft Excel in X and Y directions of the building model T4080 were shown in Charts 5 and 6. The yield point was obtained from this graph.

Meanwhile, displayed in Charts 7 and 8 are the graphs of PGA versus displacement of the building model T4080. This was used in determining the ductility factor.

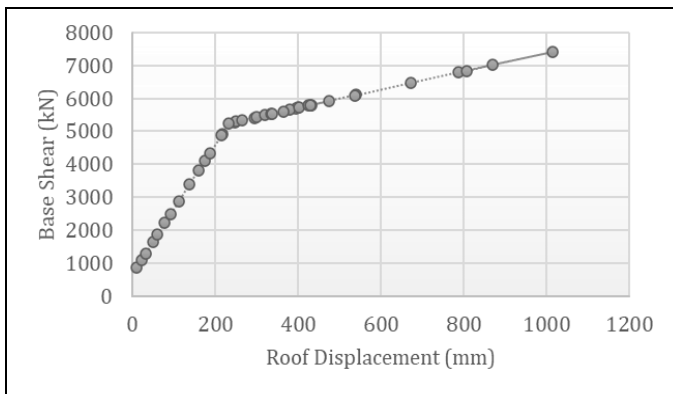


**Chart - 5:** Bilinearization for Base Shear Versus Displacement of T4080\_FC25FY420 (X Direction)

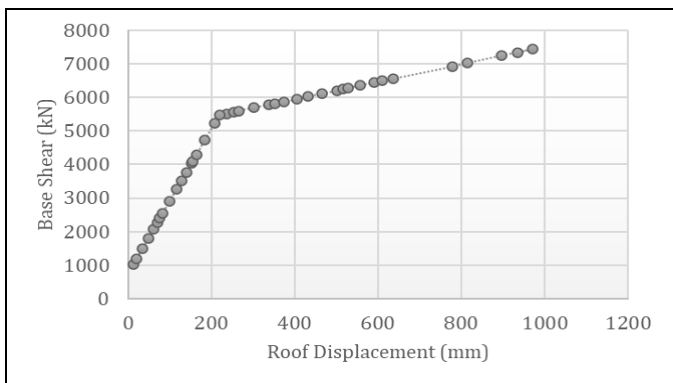


**Chart - 6:** Bilinearization for Base Shear Versus Displacement of T4080\_FC25FY420 (Y Direction)

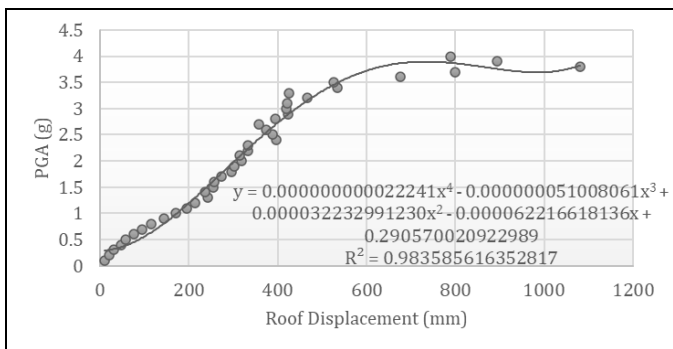


**Chart - 7:** PGA Versus Displacement of T4080\_FC25FY420 (X Direction)

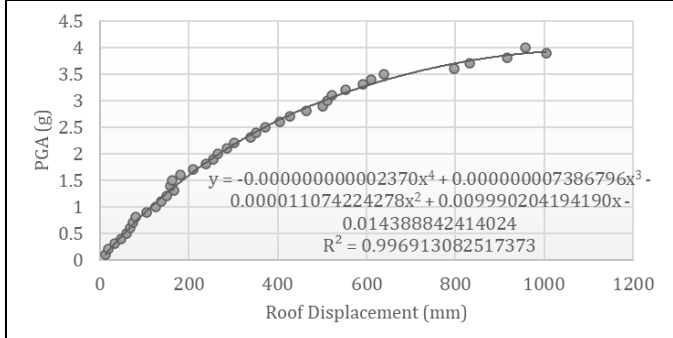


**Chart - 8:** PGA Versus Displacement of T4080\_FC25FY420 (Y Direction)

The relationship between the various parameters and ductility factors were obtained using stepwise nonlinear regression analysis. The results are shown in Tables 13 and 14, for X and Y directions, respectively. The best performing model per IV counts starting from 2 variables up to the full model, 12 variables, are chosen.

**Table - 13:** Stepwise Nonlinear Regression Results for Ductility at X Direction

IV count	Best Model	Selected IVs	R <sup>2</sup>	RMSE	MSE	MAE
2	Decision Tree	IV1, IV10	0.749	0.057	0.003	0.180
3	Decision Tree	IV1, IV5, IV10	0.844	0.042	0.003	0.180
4	Decision Tree	IV1, IV5, IV8, IV10	0.905	0.043	0.002	0.164
5	Decision Tree	IV1, IV4, IV5, IV6, IV10	0.913	0.039	0.001	0.172
6	Decision Tree	IV2, IV3, IV4, IV5, IV8, IV10	0.935	0.032	0.001	0.127
7	Decision Tree	IV1, IV2, IV3, IV4, IV5, IV8, IV10	0.948	0.041	0.001	0.153
8	Decision Tree	IV1, IV2, IV3, IV4, IV5, IV8, IV9, IV10	0.963	0.054	0.001	0.126
9	Decision Tree	IV1, IV2, IV3, IV4, IV5, IV8, IV9, IV10, IV12	0.972	0.054	0.001	0.126
10	Decision Tree	IV2, IV3, IV4, IV5, IV6, IV7, IV8, IV9, IV10, IV11	0.942	0.030	0.001	0.126
11	Decision Tree	IV2, IV3, IV4, IV5, IV6, IV7, IV8, IV9, IV10, IV11, IV12	0.946	0.030	0.001	0.122 2
12	Gaussian Process Regression	IV1, IV2, IV3, IV4, IV5, IV6, IV7, IV8, IV9, IV10, IV11, IV12	0.99	0.007	0.001	0.005

Legend: IV1 - Plan Shape; IV2 – Projection X; IV3 – Projection Y; IV4 – Building Weight; IV5 – Concrete Strength; IV6- Rebar Strength; IV7 – Shear Reinforcement in Beams; IV8 - Shear

Reinforcement in Columns; IV9 – Flexural Reinforcement in Columns; IV10 – Top Bar Reinforcement in Beams; IV11 – Bottom Bar Reinforcement in Beams; IV12 – Compression-to-Tension Reinforcement in Beams

**Table – 14:** Stepwise Nonlinear Regression Results for Ductility at Y Direction

IV count	Best Model	Selected IVs	R <sup>2</sup>	RMSE	MSE	MAE
2	Kernel Ridge	IV1, IV9	0.443	0.072	0.005	0.170
3	Kernel Ridge	IV7, IV9, IV12	0.858	0.064	0.004	0.165
4	Kernel Ridge	IV4, IV9, IV10, IV12	0.952	0.054	0.003	0.163
5	Kernel Ridge	IV4, IV5, IV6, IV9, IV12	0.940	0.060	0.004	0.161
6	Decision Tree	IV1, IV5, IV6, IV10, IV11, IV12	0.723	0.037	0.003	0.162
7	Decision Tree	IV6, IV7, IV8, IV9, IV10, IV11, IV12	0.750	0.022	0.002	0.161
8	Kernel Ridge	IV2, IV5, IV6, IV7, IV8, IV9, IV10, IV12	0.897	0.061	0.004	0.152
9	Kernel Ridge	IV1, IV3, IV4, IV5, IV6, IV7, IV9, IV11, IV12	0.999	0.052	0.003	0.123
10	Kernel Ridge	IV1, IV3, IV4, IV5, IV6, IV7, IV8, IV9, IV11, IV12	0.999	0.051	0.003	0.124
11	Kernel Ridge	IV1, IV3, IV4, IV5, IV6, IV7, IV8, IV9, IV10, IV11, IV12	0.999	0.050	0.003	0.123
12	Decision Tree	IV1, IV2, IV3, IV4, IV5, IV6, IV7, IV8, IV9, IV10, IV11, IV12	0.94	0.006	0.001	0.044

Legend: IV1 - Plan Shape; IV2 – Projection X; IV3 – Projection Y; IV4 – Building Weight; IV5 – Concrete Strength; IV6- Rebar Strength; IV7 – Shear Reinforcement in Beams; IV8 - Shear Reinforcement in Columns; IV9 – Flexural Reinforcement in Columns; IV10 – Top Bar Reinforcement in Beams; IV11 – Bottom Bar Reinforcement in Beams; IV12 – Compression-to-Tension Reinforcement in Beams

### 3.2 Development of the Regression Model

Shown in Table 14 is the results of the regression analysis using MATLAB’s Regression Learner App with 5-fold Cross validation.

**Table – 14:** Regression Models using 5-fold Cross Validation

Regression Model	Regression Type	Output	R <sup>2</sup>	RMSE	MSE	MAE
Rational Quadratic GPR	Gaussian Process Regression	Ductility at X	0.590	0.118	0.014	0.088
Optimizable Tree	Ensemble of Trees	Ductility at Y	0.170	0.153	0.023	0.111

Meanwhile, the results of the regression analysis using MATLAB’s Regression Learner App with 10% Hold-out Validation are shown in Table 15.

**Table – 15:** Regression Models using 10% Hold-out Validation

Regression Model	Regression Type	Output	R <sup>2</sup>	RMSE	MSE	MAE
Optimizable SVM	Support Vector Machine	Ductility at X	0.570	0.094	0.009	0.083
Optimizable Tree	Ensemble of Trees	Ductility at Y	0.360	0.089	0.008	0.068

To capture complex and nonlinear relationships among the data, Neural Network Fitting Tool was also used to develop a regression model estimating the ductility values in both directions.

The results of the regression analysis using neural networks considering data split of 70% Training, 15% Validation, and 15% Test sets, are shown in Table 16.

**Table – 16:** Neural Network Models

Output	Training		Validation		Test		All R
	MSE	R	MSE	R	MSE	R	
Ductility at X	0.005	0.923	0.006	0.840	0.012	0.855	0.903
Ductility at Y	0.018	0.666	0.020	0.362	0.029	0.244	0.552
Ductility at X and Y	0.015	0.820	0.015	0.762	0.016	0.807	0.808

### 3.3 Ductility Estimation of an Actual Re-entrant Corner RC Building

Shown in Table 17 is the results of the estimation of ductility of the T-shaped re-entrant corner RC building using nonlinear pushover analysis.



**Table - 17:** Ductility using Nonlinear Pushover Analysis

Method	Maximum Displacement (mm)	Yield Displacement (mm)	Displacement Ductility	Ductility
Pushover Analysis at X	169.4098	19.872	8.525	<b>4.006</b>
Pushover Analysis at Y	168.3604	24.658	6.828	<b>3.557</b>

Moreover, the results of the nonlinear time history analysis of the actual building is shown in Table 18.

**Table - 18:** Ductility using Nonlinear Time History Analysis.

Method	Maximum Displacement (mm)	Yield Displacement (mm)	PGA at max	PGA at yield	Ductility
Time History Analysis at X	336.461	113.452	1.859	0.849	<b>2.190</b>
Time History Analysis at Y	1089.899	112.460	1.496	0.729	<b>2.052</b>

The result of the ductility estimation using the developed regression model is shown in Figure 3.

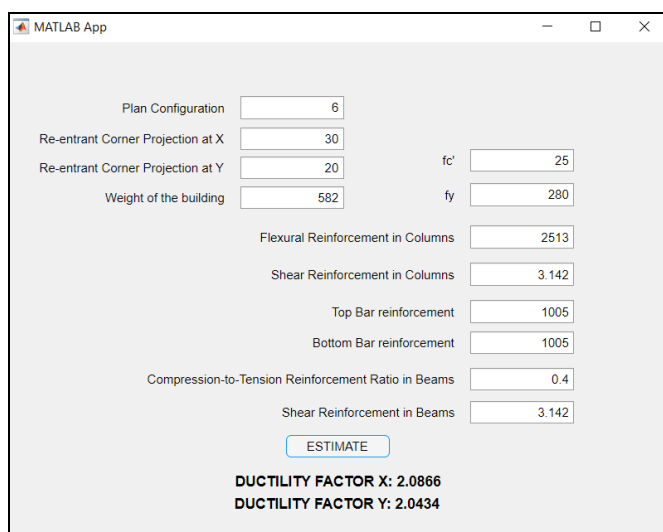


**Fig - 3:** Ductility Using the Developed Regression Model

Meanwhile, Table 19 shows the comparison of the ductility values obtained using the developed regression model

compared to the code-prescribed methods, pushover analysis and nonlinear time history analysis.

**Table - 19:** Comparison of the Ductility Values

Method	Ductility at X	Ductility at Y
Pushover Analysis	<b>4.006</b>	<b>3.557</b>
Nonlinear Time History Analysis	<b>2.190</b>	<b>2.052</b>
Developed Regression Model	<b>2.0866</b>	<b>2.0434</b>

## 4. ANALYSIS AND DISCUSSION

### 4.1 Evaluation of the Seismic Response of Re-entrant Corner RC Buildings

- Nonlinear time history analysis revealed that buildings with larger re-entrant corner projections (e.g., 80%) exhibited higher ductility, while those with smaller projections (e.g., 20%) performed less favorably. This behavior was caused by the experimental setup where all building models designed to have equal beam dimensions and equal column dimensions across the 180 building models. The key differentiating factor was the percentage of re-entrant corner projection which introduced geometric irregularity on the building models.
- Model T4080 consistently displayed the highest ductility, while models like Z2020 and Z4060 had the lowest.
- As the number of independent variables (IV) increase, the model accuracy improves significantly, from 0.749 to 0.99.
- The error metrics decreases as IV count increases. This indicates better predictive performance with more IVs.
- The variables that appear consistently across the best models per IV count indicates strong influence on the ductility on x- direction. These includes plan shape, concrete strength, top bar beam reinforcement, shear reinforcement in columns, building weight, projections in X and Y, flexural reinforcement in columns, and compression-to-tension reinforcement ratio in beams.
- Meanwhile, for ductility on y-direction, the highly influential variables are compression-to-tension reinforcement ratio, flexural reinforcement in column, rebar strength, concrete strength, top bar beam reinforcement, shear reinforcement in beam, plan shape, projection in Y, and building weight.

### 4.2 Development of the Regression Model

- The ductility at X can be estimated reliably using nonlinear techniques like Neural networks or Gaussian process regression.

- Meanwhile, the ductility at Y is more variable due to directional irregularities or less significant predictor correlation.
- The regression model predicting the combined ductility at X and Y offers good overall correlation between predicted and actual ductility values. It also generalizes well on unseen data.

#### 4.3 Ductility Estimation of an Actual Re-entrant Corner RC Building

- Ductility values are higher in pushover analysis because it uses static nonlinear loading and does not capture dynamic effects like inertia, rate of loading, or cyclic degradation.
- Time History analysis gives a more conservative ductility estimate compared to pushover analysis.
- The developed regression model provides a ductility estimate close to the results of the nonlinear time history analysis with 4.7% difference in X direction and 0.4% difference in y direction.

### 5. CONCLUSIONS

This study demonstrated how re-entrant corner projections affects significantly the ductility of reinforced concrete buildings when subjected to earthquake loads.

When all building models were designed to have equal beam dimensions and equal column dimensions, the re-entrant corner projection becomes a critical factor, where larger projections tend to improve ductility by promoting better distribution of seismic forces and energy dissipation, while smaller projections lead to stress concentration and reduced performance.

Among the models tested, T4080, T-shaped with 40% projection at X and 80% projection at Y, consistently showed superior ductility.

Through nonlinear regression, it was found that model accuracy improves as more influential variables, such as plan shape, material properties, and reinforcement details, are considered. The ductility in the X-direction can be predicted reliably, while estimates in the Y-direction show greater variability due to directional irregularities.

Moreover, the combined regression model generalized well and closely matched the results from nonlinear time history analysis, outperforming pushover estimates. This highlights the value of using data-driven approaches for practical and accurate ductility prediction in irregular RC buildings.

### REFERENCES

- [1] Philippine News Agency (PNA), "Phivolcs: PH experiences an average of 30 quakes per day," *Philippine News Agency*, Jan. 17, 2025. [Online]. Available: <https://www.pna.gov.ph/articles/1242557>.

- [2] DOST-PHIVOLCS, "Destructive Earthquake of the Philippines," [Online]. Available: <https://www.phivolcs.dost.gov.ph/index.php/earthquake/destructive-earthquake-of-the-philippines/17-earthquake>. [Accessed: Apr. 17, 2025].
- [3] D. O. Knuttunen, "The role of ductility in seismic design," *Civil Engineering Practice*, vol. 2, pp. 17-31, 1987. [Online]. Available: <https://www.bscesjournal.org/wp-content/uploads/CEP-Vol-2-No-1-02.pdf>.
- [4] R. Park, "Evaluation of ductility of structures and structural assemblages from laboratory testing," *New Zealand National Society for Earthquake Engineering*, vol. 22, no. 3, Sep. 1989.
- [5] C. Shreyasvi and B. Shivakumaraswamy, "Seismic response of buildings with re-entrant corners in different seismic zones," *IJRET: International Journal of Research in Engineering and Technology*, vol. 4, no. 4, 2015.
- [6] Association of Structural Engineers of the Philippines, *National Structural Code of the Philippines: Volume 1 – Buildings, Towers and Other Vertical Structures*, 7th ed. ASEP, 2015.
- [7] N. Dixit and A. Jhanjhot, "Analysis & design of irregular building with re-entrant corner using pushover analysis: A review," *International Journal of Scientific Development and Research (IJSDR)*, vol. 5, no. 9, 2020.
- [8] R. Riddell, P. Hidalgo, and E. Cruz, "Response modification factors for earthquake-resistant design of short period buildings," *Earthquake Spectra*, pp. 571-590, 1989.
- [9] *Applied Technology Council, Structural Response Modification Factors*, 1995.
- [10] *The Japan Building Disaster Prevention Association, Standard for Seismic Evaluation and Guidelines for Seismic Retrofit of Existing R/C Buildings (English Translation)*, 2005.
- [11] M. M. Ahmed, M. H. Baluch, A. K. Azad, and A. M. Alhozaimy, "Effect of top beam reinforcement anchorage details on the ductility of high strength concrete beam-column joints," *KSCE Journal of Civil Engineering*, vol. 23, no. 7, pp. 3096–3105, 2019, doi: 10.1007/s12205-019-1285-6.
- [12] A. K. Chopra, *Dynamics of Structures: Theory and Applications to Earthquake Engineering*, 5th ed. Pearson, 2017.

### BIOGRAPHY



**Joshua C. Junio** is a candidate for the degree, Master of Science in Civil Engineering, major in Structural Engineering, at Tarlac State University in Tarlac City, Tarlac, Philippines. He is currently a faculty member in the Civil Engineering Department at Pangasinan State University- Urdaneta City Campus in Urdaneta City, Pangasinan, Philippines.